Corrosion-Resistant Anisotropic Conductive Adhesive for Consumer Electronic Applications

Bo Xia, Jayesh Shah, Wanda O'Hara
Henkel, Corporation
46 Manning Rd.
Billerica, MA 01821
Phone: 978.436.9745, Fax: 978.436.9707
Email: bo.xia@nstarch.com, www.emersoncuming.com

Abstract

Resin-based interconnection materials for flip die technologies have been widely used in manufacturing electronic devices such as flat panel displays and other semiconductor package modules in form of (die)or chip on glass (COG) and (die) or chip on flex (COF) for the last thirty years. Traditionally, these applications used anisotropic conductive film (ACF) which enables lead(Pb)-free assembly, but requires additional handling and laminating steps. The proliferation of flip die technology is evident in many consumer electronic applications such as RFID and mobile phones, where the high throughput rate and lower processing temperature is critical. For many of these emerging applications the traditional anisotropic conductive adhesive (ACA) (mainly ACF) may not be suitable with regard to cure speed and the compatibility with non noble metallization. Customer market studies show there is a requirement for a low temperature, snap cure anisotropic conductive paste (ACP) which can be dispensed, jetted or printed on the substrate prior to the assembly.

In this paper, a novel anisotropic conductive paste (ACP) which was formulated and optimized through mixture DOE methods will be discussed. The paper will also analyze the effects of different bonding parameters, such as temperature, pressure, and curing time studied and optimized through factorial DOE methods. The paper will present details on the work life jettability, stencil and screen printing characteristics of this novel ACP. The contact resistance and adhesion strength stability of the ACP to non-noble metal (Cu, Al) in 85°C/85% RH for greater than 250 hours and 500 hours thermal shock cycles will be discussed.

Key words: RFID, anisotropic conductive adhesive, corrosion resistant

Introduction

Over the last two decades, flip die technology has been widely accepted and proven for many high end electronic devices such as flat panel displays and other semiconductor package modules in form of die on glass (COG) and die on flex (COF)[1,2]. Traditionally these applications have used anisotropic conductive film (ACF) as a means for interconnects[3].

Flip die technology continues to proliferate in many consumer electronics applications like RFID and mobile phones. Contrary to high end applications like flat panel displays, emerging consumer electronic applications like RFID pose different challenges. Although anisotropic conductive films (ACFs) provide excellent low contact resistance and compatibility with noble metallization, excellent adhesion to glass and reliable interconnect on fine resolution lines, the materials are not suitable for RFID applications because of their cost, higher cure temperature and multiple processing steps. For many low-cost applications like RFID, the interconnect adhesive needs to provide lower cost, faster throughput, lower

processing temperatures and very good compatibility with non-noble metals like etched Cu and etched Al. RFID inlay manufacturers continue to find ways to lower the cost of the tags by using lower cost substrates like PET and antenna metallization like etched aluminum, die cut aluminum and etched Cu. The most common issue with non-noble metallization is that it is prone to galvanic corrosion when subjected to high humidity and high temperature exposure [4]. This paper discusses a newly developed anisotropic conductive paste suitable for non-noble metallization commonly used for RFID antenna production.

Anisotropic conductive adhesives for RFID Interconnect Technology

Thin RFID tags are assembled by attaching a RFID die to the antenna. RFID die for RFID applications have low I/O counts (typical, 4). It can be used directly as a bare die, or be prepackaged into a die strap for easy processing.

In general, ACP materials are prepared by dispersing electrically conductive particles in an adhesive matrix. The volume fraction of particles is well below the percolation threshold (typically between 5 and 10%), thus there are no continuous conductive paths among particles in the X-Y plane. In the Z direction, electrical conduction is established by the deformation of the conductive particles trapped between die bumps and substrate pads.

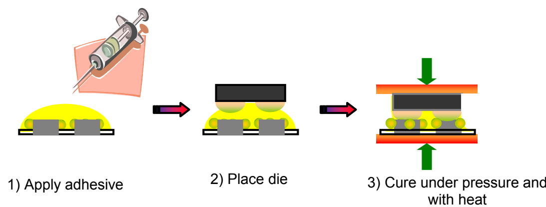

Figure 1: Schematic drawing of ACP assembly.

Figure 1 represents the common RFID inlay assembly process using ACP to assemble electrical joints between the I/O of the die and the antenna leads [5]. There are three steps in the process: (1) dispensing or screen printing of adhesive paste onto the substrate (2) pick and place dies on the adhesive; (3) thermal compression bonding to form the electrical joint.

It is critical that the ACP formulation is optimized for dispensability, adhesion, interconnect yield and reliability. The paper discusses the mixture DOE (Design of Experiments) and factorial DOE method using Stat-Ease design expert software to study the filler type, amount, rheology modifier and bonding force of these important factors. The paper will discuss the effect of these variables on the interconnect yield and reliability of RFID tags. The ACP was evaluated for dispensing using an Aysmtek DJ-9000 jet dispenser and screen printing using a commercial screen printer. Parameters of the equipment for maximum work life and yield will be discussed.

Experimental methodology:

Test vehicles:

A commercially available etched aluminum UHF antenna design as shown in figure 2 below was used. An Impinge gen-2 die with grounded path was used to assemble the RFID tags. In addition, other antenna substrates like vapor deposited aluminum and vapor deposited Cu, and etched Cu was assessed.

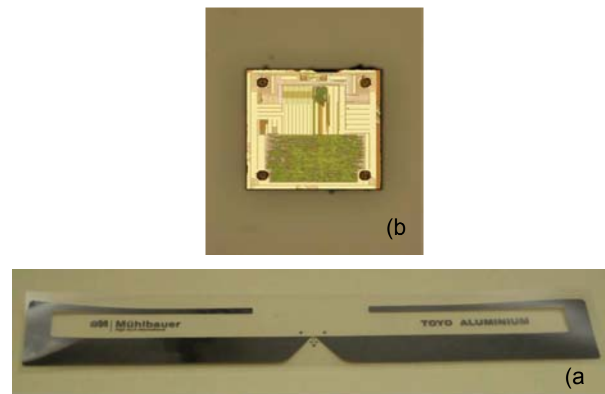

Figure 2: (a) Etched aluminum UHF antenna; (2) imping gen-2 die.

Bonding equipments and bonding condition:

A Finetech Manual Benchtop Flip Die Bonder and a Muhlbauer Die Bonder Model TTS300 were used for the placement and assembly of the RFID inlays. The bond line temperature profile is 9sec at 170C, 2N force as shown in Figure 3

Figure 3: Bonding condition profile at bond line.

Reliability tests:

The single joint contact resistance of the assembled shorted tags was measured using multimeter two probe ohmmeter. The tags were subjected to damp heat (85°C/85% RH) conditions in a humidity chamber up to two weeks and the change in contact resistance was measured. The tags were also tested for T-shock conditions (-40 to 85°C) for up to 200 cycles. Bend resistance on 1.75" diameter mandrel 40 passes with 500gram weight and change in contact resistance was measured.

Other tests included viscosity, which was measured using TA instruments Rheometer;. Die shear adhesion strength was measured with a Dage Series 4000 Bondtester. Jetting and printing evaluation details will be described in a later section.

Formulation and process study through Factorial DOE

A previously developed ACA has features such as: snap cure capability at low temperature, very strong adhesion strength on etched aluminum and copper surface, more than 48hours work life at ambient temperature, and a low interconnect contact electric resistance. However, the contact resistance on non-noble metals (Al, Cu) increased when aged in a damp heat (85°C/85%RH) environment. The rheology of the material is not suitable for jet dispensing. Design of Experiment (DOE) method was used to modify the ACA formula to overcome these drawbacks. Previous studies showed that conductive fillers play an important role on electrical contact resistance and contact resistance reliability. The process bonding force may also be a key factor. Therefore a general factorial DOE was designed and conducted to study the effect and interaction of factors like conductive filler grade and conductive filler loading, and the process factor (bonding force) on electrical contact resistance performance on etched Al after initial bonding or after damp heat aging. Table 1 shows the design layout. There are a total 20 runs, including 4 runs as repeats. Each run has 5 replicate samples. There are four filler types: filler A, filler B, filler C and filler D. Filler loading has 2 levels: low loading and high loading. Bonding force has 2 levels: 1 N and 3 N force. The electrical contact resistance (CR) before and after 85C°/85%RH was measured as main responses.

For the initial contact resistance, the statistic analysis reveals that only the bonding force is statistically significant as indicated in figure 4. The 3N force always generates lower contact resistance for all 4 filler types at both low and high loading. There is no significant difference from different filler types and filler loadings. However, for the contact resistance after 85C/85RH aging, interaction exists between the factors of filler type and bonding force as shown in figure 5 below. It is evident that the effect of changing filler type depends on different bonding force. The bar at each point indicates the least significant difference

		Factor 1	Factor 2	Factor 3
Std	Run	A:filler type	B:filler loading	C:bonding force
			%	N
8	1	filler D	high	1.5 N
13	2	filler A	high	3 N
12	3	filler D	low	3 N
15	4	filler C	high	3 N
3	5	filler C	low	1.5 N
14	6	filler B	high	3 N
10	7	filler B	low	3 N
20	8	filler D	high	3 N
4	9	filler D	low	1.5 N
6	10	filler B	high	1.5 N
9	11	filler A	low	3 N
2	12	filler B	low	1.5 N
7	13	filler C	high	1.5 N
5	14	filler A	high	1.5 N
1	15	filler A	low	1.5 N
11	16	filler C	low	3 N
19	17	filler A	high	1.5 N
18	18	filler D	high	3 N
17	19	filler C	low	1.5 N
16	20	filler B	low	1.5 N

Table 1: Factorial DOE design matrix.

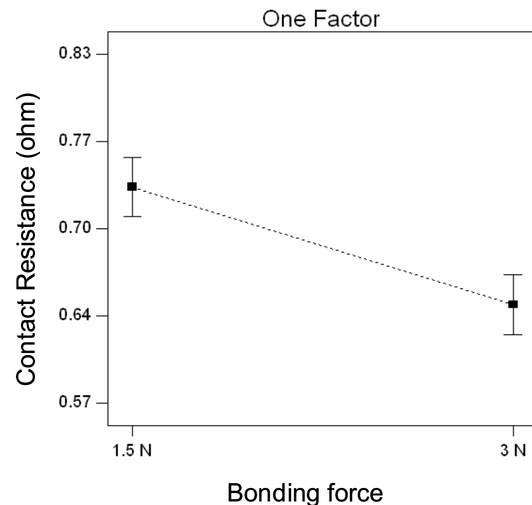

Figure 4: Plot of factor "bonding force" to "contact resistance".

(LSD) at the 95 percent confidence level. The overlap of these LSD bars at filler C indicates that it may be more robust to the process condition. Based on this DOE and consideration of filler morphology, size and surface area characteristics, the filler C was chosen for further formulation optimization.

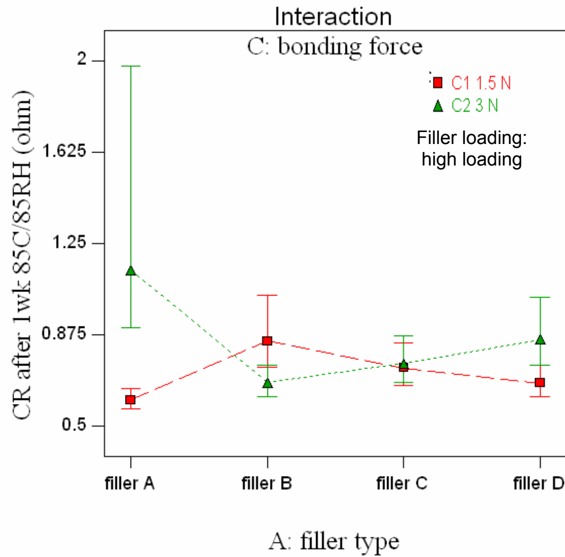

Figure 5: Plot of two factors interaction for CR after 1 wk 85C/85%RH.

Optimized formulation through mixture DOE

The factorial DOE identified filler C is the best conductive filler to offer low and stable electrical contact resistance on etched Al when bonded with low or high force. However, the formula was still not conducive to jet dispensing. The rheology of the formula still required adjustment and optimization

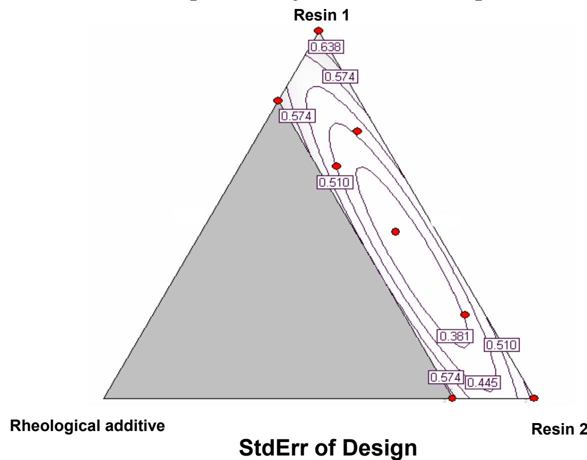

Figure 6: Location of experiment blends within feasible mixture space.

DOE	CR-initial	CR- 2wks at 85C/85%RH	Viscosity at 15S-1 at 25C	Shear thinning index	die shear strength
	ohm	ohm	pa.s		kg
1	0.72	1.44	19.24	2.80	14.70
2	0.66	0.70	16.30	2.38	15.00
3	0.74	1.10	17.30	2.59	13.60
4	0.66	2.10	16.52	2.20	14.50
5	0.64	8.83	14.03	2.26	14.50
6	0.63	1.57	19.30	3.16	15.50
7	0.59	0.94	18.13	2.84	14.90
8	0.65	0.68	21.44	2.97	13.50

Table 2: Mixture DOE data summary.

enable jet dispensing. A three component mixture DOE was designed and performed to optimize the formulation for rheological properties. The location of experiment blends within feasible mixture space is shown in figure 6. The three components are: resin 1, resin2 and a rheological additive. Resin 1 and resin 2 are very different in viscosity.

All the responses are summarized in table 2. Initial contact resistance and die shear strength are not differentiated in this mixture DOE space. The other responses are analyzed through DOE software, and significant models are found to fit the data and formulate the prediction. Since initial contact resistance and die shear adhesion strength meet the requirements within the whole design space, the optimization criteria for a desired product is focused on CR after 2 weeks 85°C/85RH, viscosity, and shear thinning index. The green area in figure 7 represents the so called "sweet spots" which indicates that the criterion is met with high desirability. The optimized formula has been proven to have good jet dispensing capability as detailed in later paragraphs.

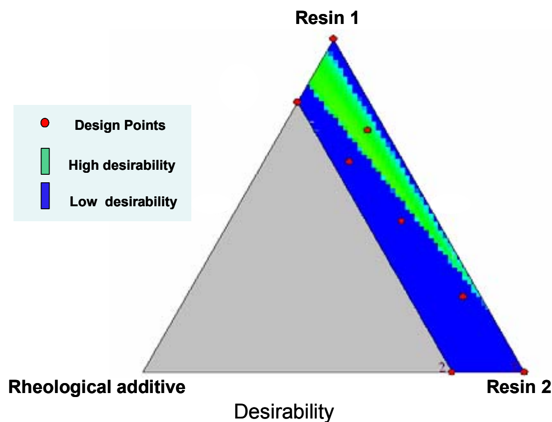

Figure 7: Meeting performance criteria --- "sweet spots" are identified.

Reliability performance

A new ACP product was developed through these factorial DOE and mixture DOE optimization processes. The new ACP offers not only good adhesion strength, snap cure capability and long work life, but also has a much improved reliability performance on non-noble metal substrates. As shown in Figure 8, a damp heat test (85°C/85%RH) and a thermal shock test were performed with the new ACP on three types of non-noble metal antennas: etched Al, etched Cu and vapor deposited Cu (VD Cu). The average contact resistance was measured before aging and after aging. The results showed the contact joint resistance remained less than 1 ohm after aging in both 85°C/85% RH up to 168 hrs and after 200 thermal shock cycles (-40°C to 85°C) .

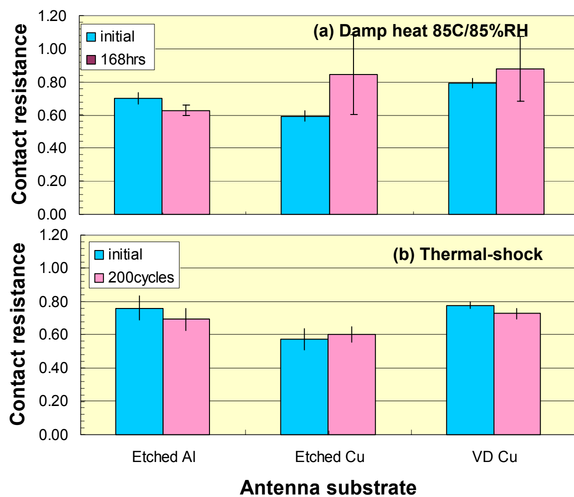

Figure 8: Contact resistance of tags before & after (a) damp heat 85C/85%RH; (b) thermal shock.

Jetting and printing study:

The stable rheology and reactivity of ACP is most critical during its work life to ensure high and reliable assembly yield. Typically, ACP products can be dispensed, jetted or printed onto the substrate. The dynamic work life of the ACP product discussed here under jetting and stencil printing was tested by means of its rheology, reactivity as function of time and its yield and reliability in 85°C/85% RH.

The print life study was conducted using an MPM Accuflex printer (shown in figure 9) over an 8hr period with continuous cycling using a demo stencil. A fixed amount of ACP was stressed under constant shear. An ACP sample was taken at different time intervals (0, 1, 2, ,4, 6 and 8 hrs) to measure reactivity by DSC, rheology, and contact resistance of assembled inlays with shorted dies.

Figure 9: MPM Accuflex printer

As shown in Figure 10, the viscosity of the ACP measured by a TA instruments AR 1000N rheometer at 1.5 sec^{-1} and 15 sec-1 after 8 hrs of constant stress shows negligible change compared to initial viscosity. Similarly, the cure kinetics measured by a differential scanning calorimeter at 10°C/min ramp rate show no change in its onset, peak exothermic temperature and enthalpy of the sample taken at t=0 and t=8 hrs suggest extremely good reactivity stability (see figure 11).

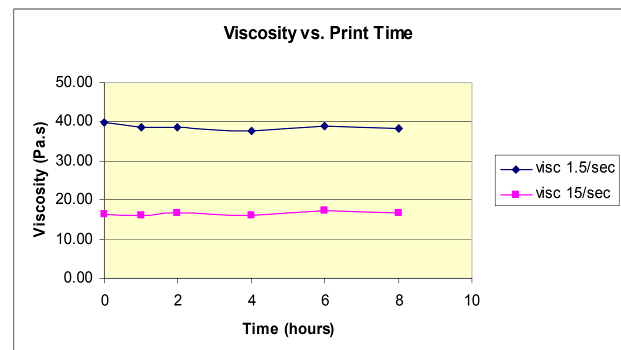

Figure 10: Print life study: viscosity vs. print time.

For evaluation of yield and reliability, material was taken from the stencil at regular intervals to build the inlays. As shown in Table 3, the contact resistance and the yield remained unaffected throughout the work life of the ACP. The data also suggests that exposure to harsh environmental conditions of 85°C/85% RH for up to seven days remains unaffected as a function of dynamic work life of the ACP. The change in contact resistance after T=8 hrs is similar to that of time zero.

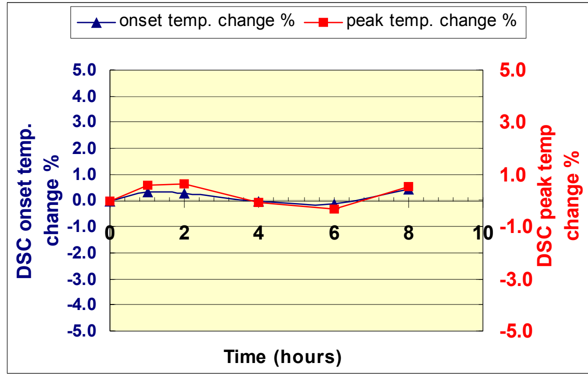

Figure 11: Print life study: DSC onset and peak temperature change vs. time.

	Aging condition 85ºC/85% RH			
	Initial (Ω)	20hr (Ω)	5 days (Ω)	7days (Ω)
0 hr	0.29	0.31	0.47	0.38
	0.27	0.27	0.45	0.39
	0.31	0.28	0.49	0.37
0 hr Ave ± S.D.	0.29 ± 0.02	0.29 ± 0.02	0.47 ± 0.02	0.38 ± 0.01
1hr	0.32	0.36	0.61	0.41
	0.3	0.28	0.45	0.39
	0.32	0.32	0.53	0.44
1 hr Ave ± S.D.	0.31 ± 0.01	0.32 ± 0.04	0.53 ± 0.08	0.41 ± 0.03
2hr	0.33	0.38	0.54	0.53
	0.31	0.3	0.51	0.47
	0.29	0.29	0.49	0.41
2 hr Ave ± S.D.	0.31 ± 0.02	0.32 ± 0.05	0.51 ± 0.03	0.47 ± 0.06
4 hr	0.31	0.31	0.43	0.37
	0.33	0.37	0.39	0.37
	0.32	0.39	0.4	0.38
4 hr Ave ± S.D.	0.32 ± 0.01	0.36 ± 0.04	0.41 ± 0.02	0.37 ± 0.01
6hr	0.33	0.41	0.39	0.35
	0.29	0.37	0.38	0.38
	0.33	0.38	0.35	0.38
6 hr Ave ± S.D.	0.32 ± 0.02	0.39 ± 0.02	0.37 ± 0.02	0.37 ± 0.02
8hr	0.29	0.37	0.35	0.38
	0.3	0.35	0.37	0.41
	0.33	0.37	0.32	0.39
8 hr Ave ± S.D.	0.31 ± 0.02	0.36 ± 0.01	0.35 ± 0.03	0.39 ± 0.02

Table 3: Contact resistance and Print life

Additionally, the screen printing was performed to assess the print definition, particles distribution and print thickness of the ACP. Screen printing was done using both 325 and 400 mesh screens with screen openings of 50 microns and 38 microns respectively. The aperture opening for the 325 mesh screen was 1.6 mm x 3 mm and the 400 mesh was 2 mm x 6 mm. There was no dragging of ACP particles and the print definition was good with both screens. The ACP thickness was measured with a Cyber Technologies Laser profilometer. The measured wet film thickness of the 325 mesh printed ACP (i.e. 1.02 mil) matched closely with the predicted wet film thickness of 1.0 mil as shown in figure 12. The same was observed with 400 mesh: the measured thickness of the ACP was 0.88 mil versus the predicted 0.8- mil.

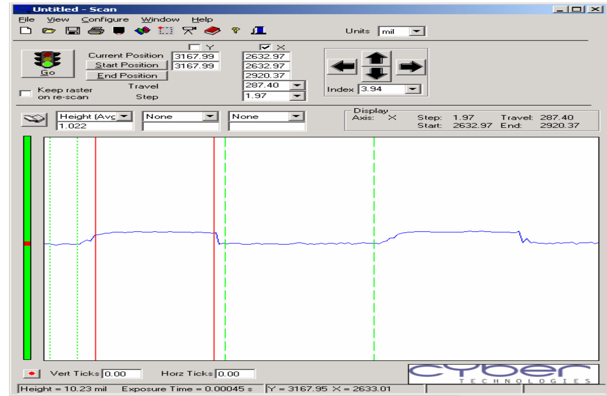

Figure 12: 325 mesh wet print thickness.

Jetting characteristics was evaluated using an Asymtek DJ9000 jet dispense pump with a unitized nozzle of 0.010" diameter and 0.030" seat with a static seal. The nozzle was heated up to 50°C and 0.8 to 1 mm dots were dispensed at 10,000 dots/hr and 40,000 dots/hr throughput rate. Dispense life was monitored for dot size consistency at 10K/hr and 40K/hr. The dot size was found to be consistent throughout 8 hours of jetting at both throughput rates of 10K/hr and 40K/hr (Figure 13), which suggests that the rheology characteristics did not change. In addition, no missing dots were found during 8 hours of jetting ACP on the substrate, which indicates material work life consistency.

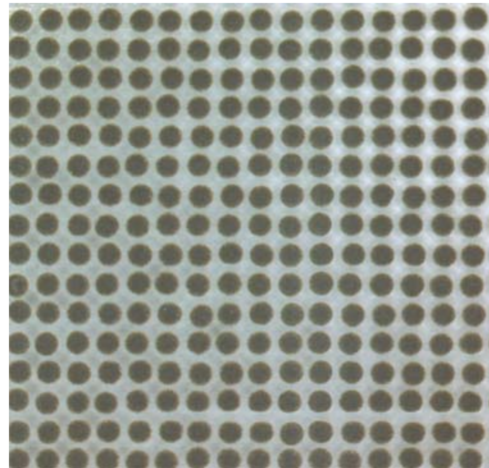

Figure 13: Jet dispensed dots are consistent in dot size.

Conclusion:

A new version of the ACP formula has been developed through a factorial DOE and a mixture DOE methodology. This snap curable product offers excellent electrical contact resistance stability with commonly used metallic antenna substrates like etched Al, VD Al and etched Cu in both thermal shock and high temperature/humidity environments. The material also has strong adhesion to various metallic antennas and provides robust mandrel bend performance. The material's rheology properties have been optimized for a wide application window and demonstrate consistent processing performance across different application methods like jet dispensing and screen printing. The continuous shearing of adhesive during a print life study did not alter reactivity or rheological properties over an 8 hour period. Assemblies of constantly sheared adhesive yielded consistent contact resistance values and stability when subsequently exposed to damp heat aging conditions.

References:

[1] A. Torri et al., "Development of Flip Chip Bonding Technology using Anisotropic Conductive Film", in Proc. 9th International Microelectronics Conference, pp. 324 ~ 327, 1996

[2] P. Clot et al., "Flip Chip on Flex for 3D Packaging", in Proc. Electronics Manufacturing Technology Symposium, 24th IEEE/CPMT, pp. 36~41, 1999

[3] Y.P.Wu et al., "Impact Properties of Flip Chip Interconnection Using Anisotropically Conductive Film on the Glass and Flexible Substrate", 2003 Electronic Components and Technology Conference, Pp.544~548

[4] J. Shah et al., "Development of isotropic Conductive Adhesive for Metallic Antenna", Smart Labels USA, March, 2006, Boston

[5] RFID tag assembly equipment using flip die assembly approach is available from
Muhlbauer AG (www.muhlbauer.com/),
Tyco Electronics (www.tycoelectronics.com/), and
Toray Engineering (www.toray-eng.com/).